Hafnium nitride films for thermoreflectance transducers at high temperatures: Potential based on heating from laser absorption

Christina M. Rost, Jeffrey Braun, Kevin Ferri, Lavina Backman, Ashutosh Giri, Elizabeth J. Opila, Jon-Paul Maria, and Patrick E. Hopkins

Citation: Appl. Phys. Lett. **111**, 151902 (2017); doi: 10.1063/1.5006648
View online: http://dx.doi.org/10.1063/1.5006648
View Table of Contents: http://aip.scitation.org/toc/apl/111/15
Published by the American Institute of Physics

Hafnium nitride films for thermoreflectance transducers at high temperatures: Potential based on heating from laser absorption

Christina M. Rost,[1] Jeffrey Braun,[1] Kevin Ferri,[2] Lavina Backman,[3] Ashutosh Giri,[1] Elizabeth J. Opila,[3] Jon-Paul Maria,[2] and Patrick E. Hopkins[1,3,4,a)]
[1]*Department of Mechanical and Aerospace Engineering, University of Virginia, Charlottesville, Virginia 22904, USA*
[2]*Department of Materials Science and Engineering, North Carolina State University, Raleigh, North Carolina 27695, USA*
[3]*Department of Materials Science and Engineering, University of Virginia, Charlottesville, Virginia 22904, USA*
[4]*Department of Physics, University of Virginia, Charlottesville, Virginia 22904, USA*

(Received 9 May 2017; accepted 20 September 2017; published online 9 October 2017)

Time domain thermoreflectance (TDTR) and frequency domain thermoreflectance (FDTR) are common pump-probe techniques that are used to measure the thermal properties of materials. At elevated temperatures, transducers used in these techniques can become limited by melting or other phase transitions. In this work, time domain thermoreflectance is used to determine the viability of HfN thin film transducers grown on SiO_2 through measurements of the SiO_2 thermal conductivity up to approximately 1000 K. Further, the reliability of HfN as a transducer is determined by measuring the thermal conductivities of MgO, Al_2O_3, and diamond at room temperature. The thermoreflectance coefficient of HfN was found to be $1.4 \times 10^{-4}\,K^{-1}$ at 800 nm, one of the highest thermoreflectance coefficients measured at this standard TDTR probe wavelength. Additionally, the high absorption of HfN at 400 nm is shown to enable reliable laser heating to elevate the sample temperature during a measurement, relative to other transducers. *Published by AIP Publishing.*
https://doi.org/10.1063/1.5006648

Thermoreflectance-based techniques such as time and frequency domain thermoreflectance (TDTR and FDTR, respectively) have emerged as powerful thermometry platforms to measure and interrogate the thermal properties of a wide range of bulk materials, nanosystems, and interfaces.[1–5] In practice, a thin metal film transducer is typically deposited on the surface of any material system to be measured with TDTR and/or FDTR in order to relate the optical reflectivity to a temperature change,[2,6] thereby relating this measured reflectivity to the thermal properties of interest. In the case of using TDTR and/or FDTR on a non-metal without the use of a metal film, the excited carrier density must be deconvolved from the measured change in reflectivity in order to accurately obtain the thermoreflectivity and thus the thermal properties of the material of interest.[7] While this process can be relatively straightforward for well-behaved materials and controlled environments, as we have demonstrated previously,[7] applying this "transducer-less" TDTR or FDTR approach to non-metals in extreme environments would be challenging due to unknowns in the electronic excitation and relaxation properties and other non-thermal-based reflectivity signals that could arise. Thus, extending these thermoreflectance-based techniques to accurately interrogate the thermal properties of materials in extreme conditions, such as ultra-high temperatures, would require the development, characterization, and calibration of thin metal film transducers that can structurally, chemically, and optically survive these environments.

However, to date, very little work has been done using TDTR/FDTR to explore thermal properties at high temperatures.[8,9] This is, in part, due to the limited number of transducer materials available that can maintain the appropriate characteristics needed at high temperature. Generally speaking, a good transducer material is the one that exhibits a high thermoreflectance coefficient at the probe wavelength, quality substrate adherence, and high thermal conductivity as not to dominate the thermal resistance driving the TDTR/FDTR signal during the measurement. Aluminum is common among metal transducers because of a high thermoreflectance coefficient around 800 nm,[10] high thermal conductivity,[11] and good substrate adherence. These positive attributes become limited at higher temperatures, as oxidation of Al is spontaneous and occurs well below the melting temperature, 660 °C.[12] Gold mitigates these issues in that it is an oxidation resistant and has a melting temperature of 1064 °C.[13] However, gold is well known for adherence issues with other materials, and low absorption at wavelengths above 700 nm (Ref. 14) makes higher pump power a requirement for reliable measurements. An obvious choice that one may consider is tungsten metal which has a melting temperature that exceeds that of HfN.[11] However, the common oxide WO_2 has a greatly reduced melting temperature of approximately 1700 °C, making ultra-high temperature testing almost prohibitively difficult.

In this paper, we demonstrate the viability of hafnium nitride (HfN) as a transducer material for TDTR/FDTR, particularly for elevated temperatures, approaching 1000 K. HfN is an electrically conductive, refractory ceramic material with a melting temperature of 3385 °C. Furthermore, the strong absorption of HfN in the visible region results in exceptionally high thermoreflectance coefficients at 800 nm,

a)Electronic mail: phopkins@virginia.edu

comparable to three materials such as Al, Ta, and, not surprisingly, TiN,[1] with the highest thermoreflectance response at 800 nm.[6] This strong visible absorption also allows for large temperature perturbations to be induced from the pump heating event during a TDTR/FDTR experiment, which opens up the possibility to control the temperature of a sample being interrogated with TDTR/FDTR using the absorbed power from the pump. This would alleviate the necessity of cumbersome sample stages to elevate the temperature of a material above ambient to measure its thermal properties. We demonstrate this "laser heating" capability in this work through the measurements of thermal conductivity of fused SiO_2 substrates with HfN transducers up to ≈1000 K. We found 1000 K to be the limiting factor for the HfN/SiO_2 system due to Hf scavenging oxygen from the SiO_2 substrate. However, with an optimized experimental setup designed such that we are able to significantly limit reactivity, the high absorption of HfN at 400 nm to facilitate "laser heating" combined with a high temperature stage will enable ultra-high temperature testing where HfN is an ideal transducer.

Thin film HfN samples were grown on c-plane sapphire, amorphous SiO_2, MgO, and diamond substrates via reactive RF sputtering using a 2-in. hafnium target in a mixed argon/nitrogen environment. Two different diamond substrates were used in this study, denoted C_{100} and C_{200} for low and high chemical purity, respectively, purchased from Element Six (Santa Clara, CA). All substrates were cleaned by a 10-min sonication in acetone followed by a sequential rinse with isopropanol and methanol and then dried under UV-Ozone exposure for 10 min. The growth conditions were optimized for maximum electrical conductivity of the HfN grown on c-sapphire, and those conditions were used for growth on subsequent substrates. Electrical conductivity was measured using a house made four-point probe setup, and the film phase and thickness were confirmed via x-ray diffraction and reflection, respectively, using a PANalytical Empyrean. Film thicknesses for each sample are summarized in Table I.

The thermal conductivities of substrates SiO_2, MgO, Al_2O_3, and diamond were determined by using a two-color TDTR setup, the details of which are described elsewhere.[2] In short, and pertinent to the current work, the TDTR system is centered around a pulsed Ti:Sapphire laser source (80 MHz, 10.5 nm bandwidth, center wavelength of 800 nm), which is split into two optical paths, the pump and the probe. The pump line is electro-optically modulated via a linearly amplified sinusoid with a frequency of 8.85 MHz and converted to $\lambda = 400$ nm using a BiB_3O_6 crystal.[15] The probe line passes through a mechanical delay stage, offsetting the arrival of the probe pulse with respect to the pump up to 5.5 ns. Both the probe and the pump are focused collinearly on the sample surface with spot radii of 4 μm and 9.5 μm, respectively. The thermal conductivities were obtained by fitting our data to a cylindrically symmetric, multi-layer thermal model described in detail elsewhere.[1,16,17] For the data analysis, we assume literature values for the temperature dependent heat capacities of the HfN transducer,[18] as well as the temperature dependent heat capacity of the substrates.[19] As we quantify later, we are relatively insensitive to the thermal conductivity of HfN. We treat the thermal conductivity of the substrate as an unknown for validation purposes. An exemplary TDTR scan of HfN on SiO_2 and its corresponding best fit model to determine the thermal conductivity, κ, of SiO_2 are shown in Fig. 1.

TABLE I. List of substrates with the corresponding HfN film thickness. All thicknesses have an uncertainty of ±2 nm.

Substrate	HfN thickness (nm)
Al_2O_3	72
SiO_2	72
MgO	70
Diamond (C_{200})	65
Diamond (C_{100})	65

In order to properly fit the data and solve for the unknown variables, it is necessary to understand the sensitivity of each variable with respect to signal output and time. Figure 2 (top) shows sensitivity curves of $-V_{in}/V_{out}$ for the HfN/SiO_2 system. The sensitivity of the TDTR measurement between 1000 and 5500 ps shows that $-V_{in}/V_{out}$ remains significant for κ_{SiO_2} while becoming insensitive to the thermal conductivity of the HfN transducer and the thermal boundary conductance at the transducer/substrate interface. Guided by this sensitivity analysis, we fit for κ_{SiO_2} using $-V_{in}/V_{out}$ between 1000 and 5500 ps. To further quantify this sensitivity, we conduct a contour plot analysis to determine the uncertainty associated with the HfN thermal conductivity. Details of this analysis are described in previous works.[20,21] As is clear from the contour plot shown in Fig. 2 (bottom), a wide range of values for the thermal conductivity of HfN can produce similar best fit results for the thermal conductivity of SiO_2 within a 95% confidence interval. We note that an analysis of the TDTR at pump-probe time delays less than 1000 ps suggests that the thermal conductivities of the HfN films are high enough to fall in this range.

Figure 3 plots the measured thermal conductivities of each substrate against their literature values using HfN as the TDTR transducer.[17,22–25] From these data, we see the expected linear relationship that strengthens the hypothesized effectiveness of HfN as a transducer to determine the thermal properties of materials using TDTR. Note that the

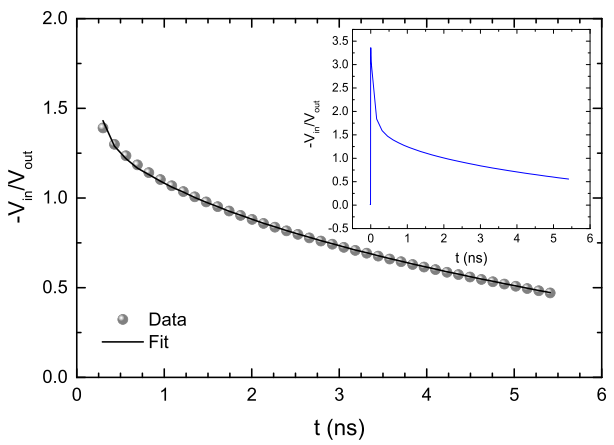

FIG. 1. Plot of the fitted ratio $-V_{in}/V_{out}$ for HfN/SiO_2. The inset shows the phase-corrected unfitted data curve.

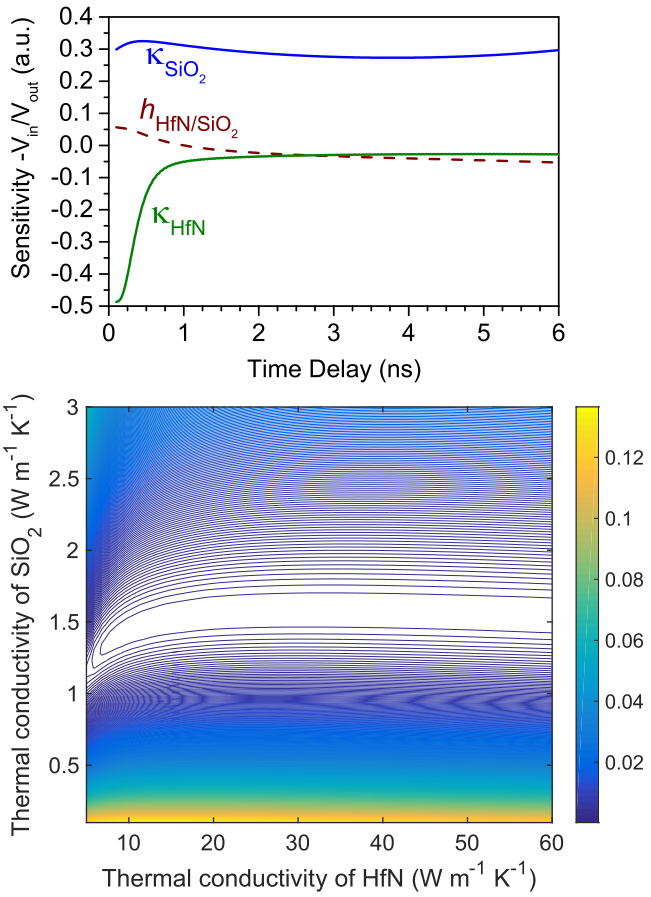

FIG. 2. Top: Sensitivity curves for $-V_{in}/V_{out}$ signals as a function of delay time between the pump and the probe for the thermal conductivities of HfN and SiO_2 and the thermal boundary conductance at the interface. Between t = 1000 and 5500 ps, it is shown that κ_{SiO_2} exhibits the highest sensitivity. Bottom: Contour plot illustrating the uncertainty of κ_{SiO_2} versus κ_{HfN}, which demonstrates that our fits are insensitive to κ_{HfN}. Note that for these calculations, ≈450 K is allowed as the sample temperature.

optical penetration depths of HfN at laser wavelengths of 400 nm and 800 nm, calculated from optical constants found in the literature,[26] are 15 nm and 27 nm, respectively. We confirm that finite optical absorption from the pump does not affect our

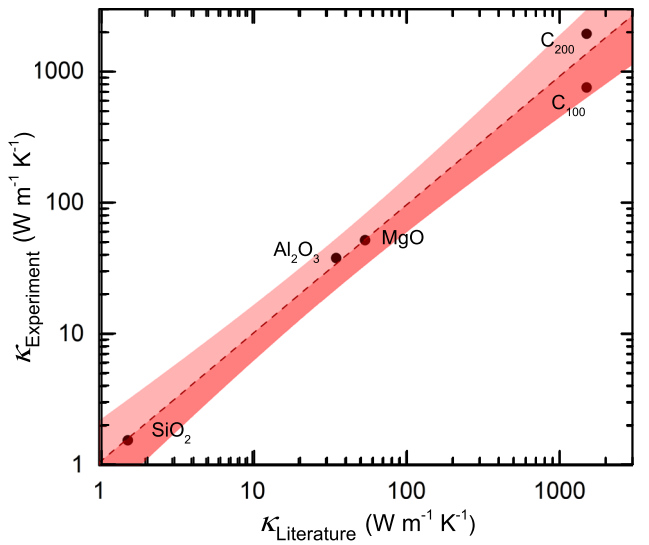

FIG. 3. Measured thermal conductivities for SiO_2, MgO, and Al_2O_3 and two qualities of diamond using a HfN transducer layer as compared to literature values. The shaded region represents 95% confidence interval.

measured thermal conductivities by repeating the HfN/SiO_2 measurements using a two-tint system (pump and probe wavelengths near 800 nm),[35] which confirmed reproducibility.

We quantified the thermoreflectance coefficient of the HfN transducers via[6]

$$\frac{dR}{dT} = \left(\frac{\sqrt{2}}{GQ}\right)\left[\frac{V(t)}{V_0}\right]\left[\frac{R}{\Delta T(t)}\right], \tag{1}$$

where $V(t)$ is the phase corrected voltage signal recorded from the lock-in amplifier, V_0 is the average DC voltage measured using the photodetector, R is the optical reflectivity of HfN near $\lambda = 800$ nm, $G = 5$ is the preamplifier gain, and $Q = 10$ is the quality factor of the system circuit. $\Delta T(t)$ is the calculated temperature induced by the pump at time t, which is detailed elsewhere.[4] We calculate dR/dT at $t = 500$ ps and perform these calculations using both the in-phase and out-of-phase signals. The results of these two calculations are then averaged in our reported values.

Using Eq. (1), we determine the magnitude of the thermoreflectance coefficient of HfN as $|dR/dT|_{HfN} = 1.4 \times 10^{-4}\,K^{-1}$ at 800 nm. In order to confirm the reliability of our dR/dT analysis, we performed the same measurement on Al and determined $|dR/dT|_{Al} = 2.3 \times 10^{-4}\,K^{-1}$ to be in good agreement with values found for Al at 785 nm.[6] We compare the thermoreflectance coefficient with those of other materials considered for TDTR/FDTR transducer applications, measured at similar wavelengths.[6] Figure 4(a) compares the thermoreflectance coefficient of HfN with that of several other transducer candidates including Ta, Al, TiN, and Au(Pd) as a function of 1-R at 800 nm. HfN is the closest in the magnitude of TiN, which has a dR/dT of $\sim 1.8 \times 10^{-4}\,K^{-1}$. Previous works[27–29] have alluded to the fact that Ta typically exhibits a crystalline phase less desirable for TDTR applications, requiring additional steps to acquire the applicable phase, while the low melting point of Al makes high temperature measurements impossible. Au(Pd) is still a promising alternative but has a thermoreflectance coefficient almost an order of magnitude smaller than that of HfN. Furthermore, the strong absorption of HfN in the visible region presents a unique advantage of HfN as a TDTR/FDTR transducer in that large temperature

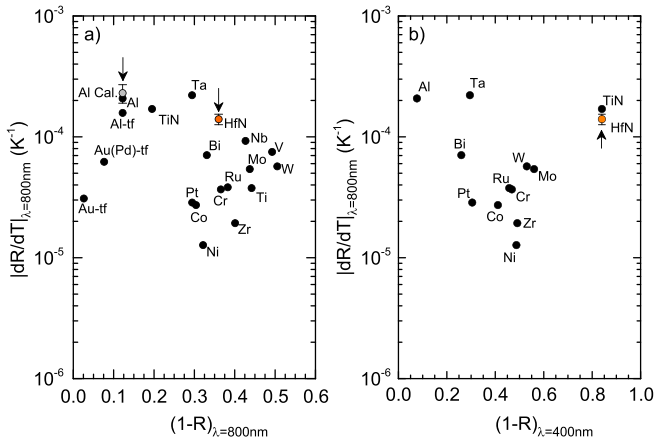

FIG. 4. Comparison of thermoreflectance coefficients of HfN with other transducer candidate systems at a probe wavelength of ≈800 nm for a pump wavelength of (a) $\lambda = 800$ nm and (b) $\lambda = 400$ nm.[6,30–34]

excursions induced from the pump could be used to elevate the local temperature of the sample in the measurement volume, if desirable. As an example of this, Fig. 4(b) plots the thermoreflectance of the elements shown in Fig. 4(a) as a function of 1-R for 400 nm. At 400 nm, a pump wavelength easily achieved by doubling the output of a Ti:Sapphire laser, HfN exhibits larger absorptivity than any other metal previously studied for TDTR optothermal transduction. This enables the possibility of elevating the sample temperature during a TDTR measurement using the absorbed energy from the pump. We discuss this in more detail later.

At this point, HfN appears to be an attractive transducer candidate to add to the growing number of usable materials for TDTR/FDTR. To test high temperature capabilities, we use a Linkam T95 heating stage to systematically increase the sample temperature under 100 sccm constant Ar flow and measure the thermal conductivity of both the SiO_2 substrate and the HfN film. Figure 5(a) plots the thermal conductivity of SiO_2 from 300 K to approximately 1000 K, where the probe signal is lost. We then compare literature values of SiO_2 with those obtained through measurements with the HfN transducer, demonstrating agreement between thermal conductivities of our measured SiO_2 and literature values,[17] further solidifying the use of HfN as a high temperature TDTR transducer.

The high absorption of HfN at 400 nm gives rise to the ability for laser-induced heating that is significantly enhanced compared to that of other typical transducer materials. For this experiment, the heating stage was kept constant at room temperature, while pump power was increased incrementally between 10 and 50 mW. The steady-state temperature rise due to laser heating is calculated using the solution to the radially symmetric heat diffusion equation (HDE) for a HfN thin film on a semi-infinite SiO_2 substrate. In this approach, we solve the HDE using a surface heat flux boundary condition based on the measured absorbance of HfN and the measured power and radius of the pump laser.[36] Because the thermal penetration depth due to the modulated heating that occurs in TDTR is much smaller than that due to the steady-state heating for the pump and probe radii used, we can estimate a constant temperature in the depth based on the surface temperature rise. We note that the thermal conductivity of SiO_2 changes with temperature; to account for this, we solve the HDE using an iterative approach, whereby we initially determine the temperature rise using room temperature thermal parameters, then adjust these parameters based on the new temperature, and repeat this process until a convergence in temperature is reached. Figure 5 shows temperature dependent thermal conductivity values of SiO_2 for direct comparison with those obtained from conventional heating and literature values. It is found that regardless of the method, κ remains consistent within the uncertainty.

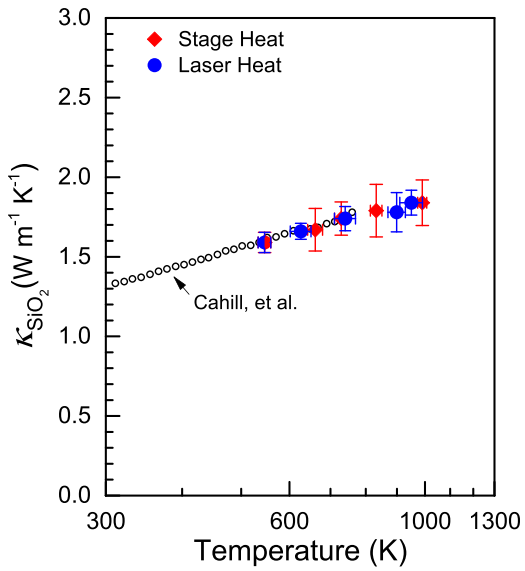

FIG. 5. Measured thermal conductivity of SiO_2 compared with known literature values. The values for both conventional and laser-induced sample heating are consistent.

As mentioned previously, the temperature-limiting factor for HfN is the propensity for Hf to oxidize, resulting in the loss of TDTR signals. Equilibrium thermodynamic calculations were performed using FactSage,[37] replicating the conditions of high temperature TDTR measurements for HfN on SiO_2. The following equilibrium phases were determined as probable given our experimental conditions assuming two situations where oxygen is or is not present within the experiment atmosphere. It should be noted that no gaseous product phases were predicted to exist above the parts per million (ppm) range.

$$4HfN_{(s)}+3SiO_{2(s)}+O_{2(g)}\rightleftharpoons 4HfO_{2(s)}+Si_3N_{4(s)}, \quad (2)$$

$$2HfN_{(s)}+2SiO_{2(s)}\rightleftharpoons 2HfO_{2(s)}+2Si_{(s)}+N_{2(g)}. \quad (3)$$

Equations (2) and (3) demonstrate that HfN will ultimately oxidize, whether through oxygen contamination of gas flow or via reaction between the film and the SiO_2 substrate. Comparing free energy of oxidation via Ellingham diagrams,[38] it becomes apparent that Hf oxidizes more readily (i.e., has a lower free energy) than Si. This, along with the FactSage calculations, supports the possibility for the transducer to scavenge oxygen from the substrate. However, both Al_2O_3 and MgO maintain a consistent lower free energy that HfO_2 up to and exceeding 1200 K, respectively. This provides a possible opportunity for pushing HfN transducers to much higher temperatures, given the proper substrates.

In summary, we have measured the temperature dependent thermal conductivity of thin film HfN up to 1000 K using TDTR. Furthermore, we have demonstrated the ability to elevate the sample temperature during a TDTR measurement via absorbed energy from the pump beam, a mechanism that is facilitated via the large optical absorption of HfN in the visible region. Regardless of thermodynamic limitations, we have added another material to the list of effective transducers for TDTR, expanding the potential for more thermal measurements in extreme temperature environments.

We acknowledge the financial support from the Office of Naval Research MURI program (Grant No. N00014-15-1-2863).

[1]D. G. Cahill, W. K. Ford, K. E. Goodson, G. D. Mahan, A. Majumdar, H. J. Maris, R. Merlin, and S. R. Phillpot, J. Appl. Phys. **93**, 793 (2003).
[2]A. J. Schmidt, Annu. Rev. Heat Transfer **16**, 159 (2013).

[3]D. G. Cahill, P. V. Braun, G. Chen, D. R. Clarke, S. Fan, K. E. Goodson, P. Keblinski, W. P. King, G. D. Mahan, A. Majumdar, H. J. Maris, S. R. Phillpot, E. Pop, and L. Shi, Appl. Phys. Rev. **1**, 011305 (2014).
[4]D. G. Cahill, Rev. Sci. Instrum. **75**, 5119 (2004).
[5]A. J. Schmidt, R. Cheaito, and M. Chiesa, J. Appl. Phys. **107**, 024908 (2010).
[6]Y. Wang, J. Y. Park, Y. K. Koh, and D. G. Cahill, Journal Appl. Phys. **108**, 043507 (2010).
[7]L. Wang, R. Cheaito, J. L. Braun, A. Giri, and P. E. Hopkins, Rev. Sci. Instrum. **87**, 094902 (2016).
[8]E. Bozorg-Grayeli, Z. Li, M. Asheghi, G. Delgado, A. Pokrovsky, M. Panzer, D. Wack, and K. E. Goodson, Appl. Phys. Lett. **99**, 261906 (2011).
[9]J. Ravichandran, W. Siemons, D. W. Oh, J. T. Kardel, A. Chari, H. Heijmerikx, M. L. Scullin, A. Majumdar, R. Ramesh, and D. G. Cahill, Phys. Rev. B **82**, 165126 (2010).
[10]R. B. Wilson, B. A. Apgar, L. W. Martin, and D. G. Cahill, Opt. Express **20**, 28829 (2012).
[11]D. Lide, *CRC Handbook for Chemistry and Physics. Internet Version*, 89th ed. (CRC Press/Taylor and Francis, Boca Raton, 2008).
[12]R. O. Simmons and R. W. Balluffi, Phys. Rev. **117**, 52 (1960).
[13]P. Buffat and J. P. Borel, Phys. Rev. A **13**, 2287 (1976).
[14]O. Loebich, Gold Bull. **5**, 2 (1972).
[15]M. Ghotbi, M. Ebrahim-Zadeh, A. Majchrowski, E. Michalski, and I. V. Kityk, Opt. Lett. **29**, 2530 (2004).
[16]A. J. Schmidt, M. Chiesa, X. Chen, and G. Chen, Rev. Sci. Instrum. **79**, 064902 (2008).
[17]D. G. Cahill, Rev. Sci. Instrum. **61**, 802 (1990).
[18]H. Marcus, "Project 7360: Chemistry and Physics Materials, Task No. 73603: Thermodynamics and Heat Transfer," Technical Report TR 60-924, Southern Research Institute under USAF Materials and Processes Directrate, 1960.
[19]Y. S. Touloukian, S. C. Saxens, and P. Hestermans, "Thermophysical properties of matter," Technical Report A129114, New York, 1975.
[20]J. P. Feser and D. G. Cahill, Rev. Sci. Instrum. **83**, 104901 (2012).
[21]A. Giri, J.-P. Niemelä, C. J. Szwejkowski, M. Karppinen, P. E. Hopkins, A. Giri, J.-P. Szwejkowski, C. J. Karppinen, M. Hopkins, C. J. Szwejkowski, and M. Karppinen, Phys. Rev. B **93**, 024201 (2016).
[22]A. M. Hofmeister, Phys. Chem. Miner. **41**, 361 (2014).
[23]G. A. Slack, Phys. Rev. **126**, 427 (1962).
[24]K. E. Meyer, R. Cheaito, E. Paisley, C. T. Shelton, J. L. Braun, J.-P. Maria, J. F. Ihlefeld, and P. E. Hopkins, J. Mater. Sci. **51**, 10408 (2016).
[25]R. M. Costescu, M. A. Wall, and D. G. Cahill, Phys. Rev. B **67**, 54302 (2003).
[26]M. Strømme, R. Karmhag, and C. G. Ribbing, Opt. Mater. **4**, 629 (1995).
[27]P. Catania, J. P. Doyle, and J. J. Cuomo, J. Vac. Sci. Technol., A **10**, 3318 (1992).
[28]D. W. Face and D. E. Prober, J. Vac. Sci. Technol., A **5**, 3408 (1987).
[29]S. Sato, Thin Solid Films **94**, 321 (1982).
[30]A. D. Rakic, A. B. Djurisic, J. M. Elazar, and M. L. Majewski, Appl. Opt. **37**, 5271 (1998).
[31]P. Johnson and R. Christy, Phys. Rev. B **9**, 5056 (1974).
[32]M. Querry, "Optical constants of minerals and other materials from the millimeter to the ultraviolet," Technical Report CRDEC-CR-88009, 1986.
[33]W. S. M. Werner, K. Glantschnig, and C. Ambrosch-Draxl, J. Phys. Chem. Ref. Data **38**, 1013 (2009).
[34]M. Polyanskiy, https://refractiveindex.info/ for "Refractive index database."
[35]K. Kang, Y. K. Koh, C. Chiritescu, X. Zheng, and D. G. Cahill, Rev. Sci. Instrum. **79**, 114901 (2008).
[36]J. L. Braun and P. E. Hopkins, J. Appl. Phys. **121**, 175107 (2017).
[37]C. Bale, E. Belisle, P. Chartrand, S. Decterov, G. Eriksson, A. Gheribi, K. Hack, I. Jung, Y. Kang, J. Melancon, A. Pelton, S. Petersen, C. Robelin, J. Sangster, and M.-A. Van Ende, CALPHAD **54**, 35 (2016).
[38]H. Ellingham, J. Soc. Chem. Ind. **10**, 125 (1944).